PROCEEDINGS of the
23rd International Congress on Acoustics
9 to 13 September 2019 in Aachen, Germany

Numerical simulation of nonlinear viscothermal acoustic wave propagation

Jan Albertus DE JONG[(1)], Erwin Reinder KUIPERS[(2)]

[(1)]ASCEE, The Netherlands, j.a.dejong@ascee.nl
[(2)]Sonova AG, Switzerland, erwin.kuipers@sonova.com

Abstract

Behind-The-Ear (BTE) hearing instruments are typically applied to assist people with a severe to profound hearing loss. Accordingly, very high acoustic pressure levels can be obtained in the ear canal of the wearer. At such levels, significant distortion is present, leading to a reduced sound quality. The distortion mainly originates from the balanced armature receiver driver, operated beyond its linear limit. However, as the acoustic pressure level in the acoustic transmission system (basically a set of tubes) can be much higher than 140 dB SPL, it is of interest to investigate the amount of acoustic distortion caused by nonlinear wave propagation.

As such, this paper focuses on the prediction of the distortion due to the combined effect of viscothermal and nonlinear wave propagation. To simulate these effects in the tubes, a modified form of the model of Chester is used. In this modified model, the viscothermal effects results in a half order derivative of the acoustic pressure to time. This fractional derivative term is approximated using the diffusive approximation, where attention is given to the linear wave dispersion error. The correct implementation of the model is verified using a 2D full nonlinear compressible Computational Fluid Dynamics simulation.

Keywords: Nonlinear, viscothermal, duct acoustics

1 INTRODUCTION

To transport the amplified signal from the receiver to the inner ear, a BTE hearing aid instrument uses several tubes with relatively small diameter, in the order of 1 mm. Due to these small channels, the acoustic wave propagation is subject to viscothermal losses. Moreover, for high amplitudes nonlinear effects can result in additional distortion of the wave signal. The combined effects of high-amplitude nonlinearities and viscothermal losses have the potential to deteriorate the speech intelligibility. Therefore, for hearing aid instrument manufacturers it is of importance to understand the combined impact of these effects. One way to get more insight into the combined effects is by utilizing a full Computational Fluid Dynamics (CFD) simulation. This often involves a too high computational cost. Hence, more simplified model is required. The focus in this work is on the derivation and implementation of a one-dimensional model for nonlinear and viscothermal acoustic wave propagation in these tubes.

The first one-dimensional (1D) nonlinear model which both incorporates viscothermal and nonlinear effects has been developed by Chester [2]. This model is based on the boundary layer approximation, i.e. the viscous boundary layer δ_ν [11] is small compared to the hydraulic radius of the tube. It is not our intention to provide a complete overview of existing efforts in this subject. However, as a good starting point, we would like to refer the reader to the work of Menguy and Gilbert [9] and Sugimoto and Shimizu. [10].

In these models, the viscothermal effects return either into the governing continuity equation, or in the governing momentum equation in the form of a fractional order derivative. A fractional order derivative is non-local in time, and requires the full time history of the computation to evaluate.

This is problematic in a numerical simulation, as the required amount of memory for the solution will grow linearly with the simulated time. As a solution to this problem, Haddar et al. [4] proposed a "diffusive approximation" to the fractional derivative. Using this diffusive approximation, the evaluation of the fractional derivative becomes again local in time, at the cost of the evaluation of extra degrees of freedom (DOFs) per grid point. Fortunately, the amount of extra DOFs is low. It should be noted that for boundary layers which are thick compared to the hydraulic radius, the fractional order derivative introduces a dispersion error, as it is derived by assuming a thin boundary layer in the first place.

In this work, we will improve upon the evaluation of the diffusive approximation to minimize this dispersion error for small tubes, especially at low frequencies. The 1D numerical model is implemented in a general framework for Finite Element Analysis (FEA) and results are compared to a full nonlinear CFD simulation.

In the next section, we will present the 1D model and its major assumptions. Using a dispersion analysis we will show how to obtain required quadrature coefficients of the diffusive approximation. We will shortly discuss the implementation of the 1D model. Section 3 provides a comparison of results for this 1D model with 2D CFD results. We will finish with some conclusions and remarks on future work in Section 4.

2 1D MODEL

Upon applying the following assumptions to the full compressible Navier Stokes equations for a calorically perfect gas [7]:

- Laminar flow,
- Prismatic duct,
- Isothermal walls,
- Large aspect ratio (length in wave propagation direction, L is much larger than transverse length scale (hydraulic radius, r_h),
- Hydraulic radius is much larger than viscous and thermal penetration depth [11, p. 7],
- In the viscothermal boundary layer, viscous effects dominate the flow and nonlinear effects are negligible, whereas in the main flow region, the viscous effects are negligible and nonlinear effects can be of importance,

we can reduce the full system of equations to the following closed set of equations for the area-averaged velocity $u(x,t)$, and area-averaged pressure $p(x,t)$ [10]:

$$\rho_0 \left(\frac{p}{p_0}\right)^{\frac{1}{\gamma}} \left(\frac{\partial u}{\partial t} + u\frac{\partial u}{\partial x}\right) + \frac{\partial p}{\partial x} = 0, \tag{1}$$

$$\frac{1}{\gamma p}\left(\frac{\partial p}{\partial t} + u\frac{\partial p}{\partial x}\right) + \frac{\partial u}{\partial x} + C\frac{\partial^{\frac{1}{2}} p}{\partial t^{\frac{1}{2}}} = 0, \tag{2}$$

where ρ_0 is the density of the gas in quiescent conditions, p_0 the atmospheric mean pressure, γ the ratio of specific heats, t time, x the coordinate in the direction of the duct length and C is defined as:

$$C = \left(1 + \frac{\gamma - 1}{\sqrt{\mathrm{Pr}}}\right) \frac{\sqrt{\nu_0}}{r_h \rho_0 c_0^2}, \tag{3}$$

in which Pr is the Prandtl number, ν_0 the kinematic viscosity at quiescent conditions, and c_0 the speed of sound at quiescent conditions. The hydraulic radius is formally defined as $r_h = S/\Pi$, where

S is the duct cross sectional area, and Π the wetted perimeter. For a circular duct with radius R, $r_h \equiv R/2$. $\frac{\partial^{\frac{1}{2}} p}{\partial t^{\frac{1}{2}}}$ is the half-order derivative of the pressure to the time, which is defined as

$$\frac{\partial^{\frac{1}{2}} p}{\partial t^{\frac{1}{2}}} \equiv \frac{1}{\sqrt{\pi}} \int_0^t \frac{1}{\sqrt{t-\tau}} \frac{\partial p}{\partial t} \mathrm{d}\tau. \tag{4}$$

In Eq. 4, it is assumed that $p(x,t<0)=0$. To compute the current value of $\partial^{\frac{1}{2}} p/\partial t^{\frac{1}{2}}$, the complete time history of $p(t)$ is required. As discussed in the introduction, this is an undesired property for numerical computations. In the next section, we will treat an implementation which solves this problem.

2.1 IMPLEMENTATION OF THE FRACTIONAL ORDER DERIVATIVE

Following Lombard and Matigon [8], a transformation can be made to write the fractional derivative as

$$\frac{\partial^{\frac{1}{2}} p}{\partial t^{\frac{1}{2}}} = \int_{\theta=0}^{\infty} \phi(t,\theta) \mathrm{d}\theta, \tag{5}$$

where ϕ satisfies

$$\frac{\partial \phi}{\partial t} = -\theta^2 \phi + \frac{2}{\pi} \frac{\partial p}{\partial t}, \tag{6}$$

with $\phi(t=0,\theta)=0$. This is called the diffusive representation of the fractional derivative, due to the similarity of Eq. 6 with, for example, Newton's cooling law. On first sight, the main advantage is that the evolution of ϕ is local in time (it contains only integer-order derivatives). And in case of a second order finite difference scheme, only the previous time instance is required to be kept in memory. However, to compute $\partial^{\frac{1}{2}} p/\partial t^{\frac{1}{2}}$ requires the computation of an improper integral in the θ-space.

In the diffusive approximation, the improper integral is estimated using a quadrature rule, on a fixed set of L points:

$$\int_{\theta=0}^{\infty} \phi(t,\theta) \mathrm{d}\theta \approx \sum_{\ell=0}^{L-1} \mu_\ell \phi_\ell(t), \tag{7}$$

where μ_ℓ are the quadrature coefficients. Now, ϕ_ℓ evolves according to:

$$\frac{\partial \phi_\ell}{\partial t} = -\theta_\ell^2 \phi_\ell + \frac{2}{\pi} \frac{\partial p}{\partial t}, \quad \ell = 0...L-1, \tag{8}$$

subject to the boundary condition at $t=0$:

$$\phi_\ell(t=0) = 0, \quad \ell = 0...L-1. \tag{9}$$

Now, the challenge is to find a proper set quadrature coefficients and points (μ_ℓ, θ_ℓ) for the estimation of the integral of Eq. 5. Here, a trade-off has to be made between computational efficiency and accuracy, as the higher L, the more variables need to be solved at each grid and time point in the numerical scheme.

2.2 Diffusive approximation quadrature coefficients

Following Lombard, we could determine the quadrature coefficients by minimizing the dispersion error between the exact frequency domain fractional order derivative and the diffusive approximation.

However, it is found that by doing this, for low frequencies, this results in a larger dispersion error, when comparing to the viscothermal wave number. Notably, it is found that for tubes with a diameter of 1 mm, this leads to a factor of 2 too low imaginary part of the wave number. The imaginary part of the wave number is related to the damping of the acoustic waves. Therefore, we propose to minimize the difference between the exact viscothermal wave number and the viscothermal wave number based on the diffusive approximation.

By substituting the x-derivative of the small amplitude linearized version of Eq. 2 into the time-derivative of the small amplitude linearized version of Eq.1 we can derive the following (lossy) 1D wave equation:

$$\frac{1}{c_0^2}\frac{\partial^2 p}{\partial t^2} - \frac{\partial^2 p}{\partial x^2} + \left(1 + \frac{\gamma - 1}{\sqrt{\mathrm{Pr}}}\right)\frac{\sqrt{\nu_0}}{r_h c_0^2}\frac{\partial}{\partial t}\frac{\partial^{\frac{1}{2}} p}{\partial t^{\frac{1}{2}}} = 0, \tag{10}$$

where Pr denotes the Prandtl number. Upon transforming Eq. 10 to the frequency domain using $e^{+i\omega t}$-convention, we can derive the following Helmholtz-like ordinary differential equation:

$$\frac{\mathrm{d}^2 \hat{p}}{\mathrm{d}x^2} + k^2\left[1 + \left(1 + \frac{\gamma - 1}{\sqrt{\mathrm{Pr}}}\right)\frac{1}{r_h}\sqrt{\frac{\nu_0}{i\omega}}\right]\hat{p} = 0, \tag{11}$$

where $\hat{p}(\omega)$ is the Fourier transform of the acoustic pressure, $k = \omega/c_0$ and $i = \sqrt{-1}$. Here, the term in front of $\hat{p}$ can be recognized as an approximation to the square of the viscothermal wave number: $\Gamma^2_{\mathrm{approx}}$. Applying the Fourier transform to Eqs. 7-8, it is found that the diffusive approximation has the following frequency domain representation:

$$\mathscr{F}\left[\sum_{\ell=0}^{L-1}\mu_\ell \phi_\ell(t)\right] \equiv \tilde{\chi}(\omega)\hat{p}(\omega) = \sum_{\ell=0}^{L-1}\frac{2i\omega}{\pi}\frac{\mu_\ell}{\theta_\ell^2 + i\omega}\hat{p}(\omega), \tag{12}$$

where $\mathscr{F}$ denotes the Fourier transform operator. Hence, in the diffusive approximation, we can derive that the viscothermal wave number will be estimated as

$$\Gamma_{\mathrm{approx}}(\omega) = k\sqrt{1 + \left(1 + \frac{\gamma - 1}{\sqrt{\mathrm{Pr}}}\right)\frac{\sqrt{\nu_0}}{i\omega r_h}\tilde{\chi}(\omega)}. \tag{13}$$

For circular ducts, an exact solution (in the low reduced frequency limit) for this viscothermal wave number is available for the viscothermal wave number, which reads [12, 3]:

$$\Gamma_{\mathrm{circ}} = k\sqrt{\frac{1 + (\gamma - 1)f_\kappa}{1 - f_\nu}}. \tag{14}$$

where

$$f_j = \frac{J_1\left[(i-1)\frac{2r_h}{\delta_j}\right]}{(i-1)\frac{r_h}{\delta_j}J_0\left[(i-1)\frac{2r_h}{\delta_j}\right]}, \tag{15}$$

in which J_n is the cylindrical Bessel function of the first kind n^{th} order and δ_ν, δ_κ are the viscous and thermal penetration depth's, respectively. They are defined as:

$$\delta_\kappa = \sqrt{\frac{2\kappa_0}{\rho_0 c_p \omega}} \quad ; \quad \delta_\nu = \sqrt{\frac{2\mu_0}{\rho_0 \omega}}, \tag{16}$$

where κ_0 is the thermal conductivity at quiescent conditions, c_p the specific heat at constant pressure, and μ_0 the dynamic viscosity at quiescent conditions.

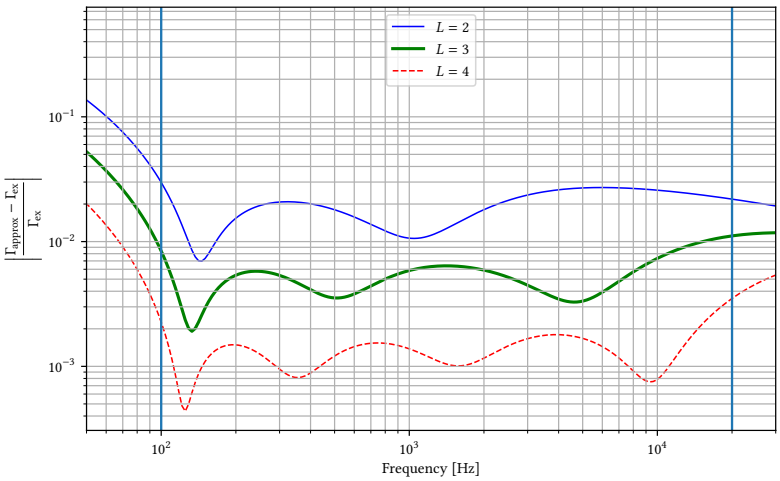

Figure 1. Normalized error in the viscothermal wave number of the diffusive approximation with optimized coefficients for μ_ℓ and θ_ℓ according to the objective function of Eq. 18, for different values of L. The tube has a diameter of 1 mm ($r_h = 0.25$ mm).

To find a set of quadrature coefficients, a set K frequencies ω_k, spanning the range from $f_0 = 100$ Hz to $f_{K-1} = 20$ kHz is chosen, which are logarithmically spaced over this range, according to

$$f_k = 100 \left(\frac{20 \cdot 10^3}{100} \right)^{\frac{k}{K-1}}.$$

Next, the quadrature coefficients are obtained by minimization of the objective function $\mathscr{J}$:

$$(\mu_\ell, \theta_\ell) = \left\{ (\mu_\ell, \theta_\ell) \,|\, \min_{\mu_\ell, \theta_\ell} \mathscr{J}(\mu_\ell, \theta_\ell) \right\}, \tag{17}$$

where the objective function is defined as

$$\mathscr{J}(\mu_\ell, \theta_\ell) = \sum_{k=0}^{K-1} \left| \frac{\Gamma^2_{\text{approx}}(\omega_k)}{\Gamma^2_{\text{circ}}(\omega_k)} - 1 \right|, \tag{18}$$

To solve this nonlinear least squares problem, we have used the Trust Region Reflective algorithm, as implemented in SciPy v1.2.1 [6]. The found optimal coefficients are dependent on L and K. It is found that for increasing K, the found coefficients μ_ℓ and θ_ℓ converge to a certain value for given L. For $K \approx 50$, the optimal values for μ_ℓ and θ_ℓ are approximately independent of K.

Figure 1 shows the error in the wave number Γ as a function of frequency for different values of L. As visible in this result, for $L = 4$, the error can be kept lower than 0.3% in the frequency range of 100 Hz to 20 kHz.

It should be noted that the found coefficients which minimize the dispersion error are dependent on the the hydraulic radius of the duct. This is due to the r_h in the denominator in Eq. 13.

2.3 Numerical implementation of the 1D model

The 1D model has been implemented in numerical code which uses the FEniCS project [1] general finite element framework. In this framework, the weak formulation of the 1D model is implemented

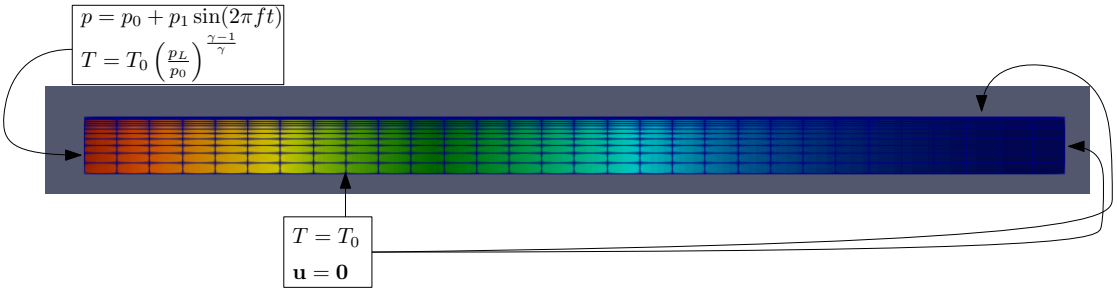

Figure 2. Schematic of the resonator geometry for CFD computations, including annotations of the boundary conditions. For visibility, the y-scale is multiplied by a factor of 100.

using a quadratic shape functions and second order implicit time-stepping procedure and constant time steps, for the variables p, u, and $\phi_0 \ldots \phi_3$. To solve the nonlinear problem at each time step, the Newton-Raphson algorithm is used.

3 COMPARISON WITH CFD RESULTS: $\lambda/4$ RESONATOR

In this section, we compare results of the 1D model with the full nonlinear compressible Navier-Stokes model (CFD). To this end, a 2D duct has been generated with a length L corresponding to a quarter wavelength: $L = \lambda/4$, where $\lambda = c_0/f$.

3.1 CFD model

We solve the full nonlinear system of equations using the `rhoPimpleFoam` solver, from the OpenFOAM CFD suite, version 6.2 [5]. Figure 2 shows the geometry, including boundary conditions. On the left side, the pressure perturbation is prescribed as a sinusoidal function of time. The according temperature is computed using the adiabatic compression/expansion relation. The velocity is computed from the model using a `pressureInletOutletVelocity` boundary condition. As a result, the duct is driven in its $\lambda/4$ resonance, leading to a high amplitude (at least according to linear isentropic acoustics) on the right side of the duct. The resulting amplitude on this side of the duct is limited by the viscothermal and nonlinear effects.

The grid typically has 30 nodes in the x-direction, and approximately 12 nodes in the y-direction. Attention has been given to put enough grid points in the viscothermal boundary layer. A grid study has been performed to check for near grid-independence of the result. For the CFD model, it was found that the time step has a strong influence on the amplitude computed on the right side. This imposed a stronger restriction on the time step than the restriction based on the CFL condition. The time step in these simulations is set to 0.1 µs.

3.2 1D model

As we are comparing for a 2D model, for the 1D model, the quadrature coefficients are determined by using the parallel-plate formulation of the viscothermal Rott functions:

$$f_j = \frac{\tanh\left((1+i)\, r_h/\delta_j\right)}{(1+i)\, r_h/\delta_j}, \tag{19}$$

which lead to slightly different values of μ_ℓ and θ_ℓ. We checked that the error we make with Γ_{approx} is in the same order as for the circular duct case. The time step has been chosen equal to the time step used in the CFD computations, and the number of grid points equal to the number in

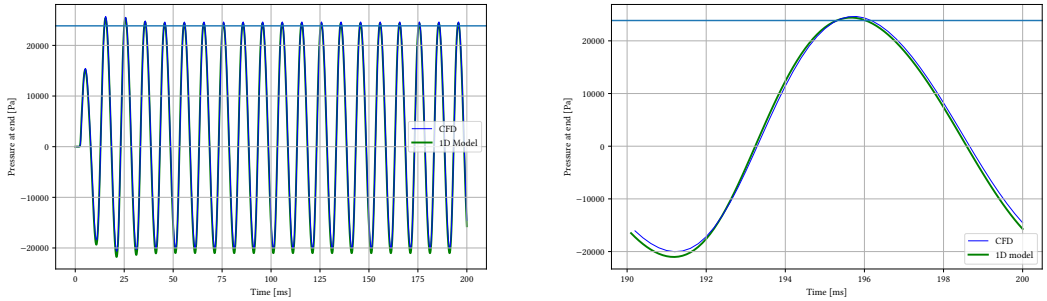

Figure 3. Comparison of the pressure perturbation response at the right side of the resonator, for $p_1 = 10,000$ Pa, and $f = 100$ Hz. Left: result over the full simulation time. Right: zoom in on the last period. The horizontal blue line denotes the pressure amplitude according to the Low Reduced Frequency theory.

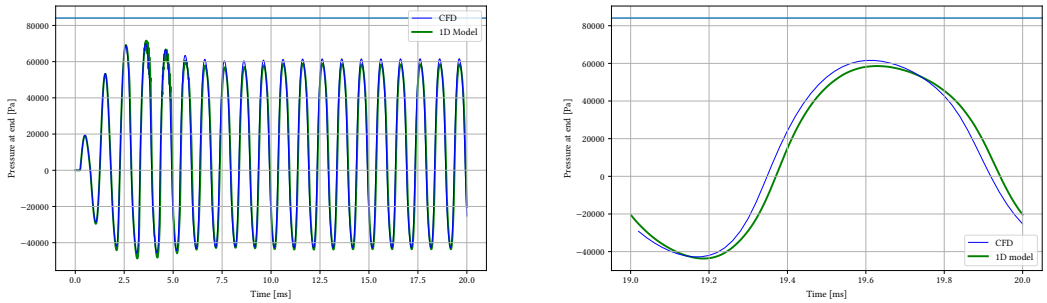

Figure 4. Comparison of the pressure perturbation response at the right side of the resonator, for $p_1 = 10,000$ Pa, and $f = 1000$ Hz. Left: result over the full simulation time. Right: zoom in on the last period. The horizontal blue line denotes the pressure amplitude according to the Low Reduced Frequency theory.

the x-direction of the CFD model.

3.3 Results

We compare results for the computed pressure perturbation on the right side of the resonator, due to pressure perturbation amplitude p_1 on the left side. The number of periods has been chosen to find a sufficiently periodic steady state. Due to the relatively high viscothermal damping, approximately 20 periods are sufficient to reach periodic steady state. The amplitude of p_1 is set to $1{\cdot}10^4$ Pa, which is such high that we expect nonlinear effects to impact the result. Figure 3 compares the result for 100 Hz. As visible, the amplitudes at the right side match quite well. As a reference, the horizontal blue line denotes the amplitude expected from Low Reduced Frequency (LRF) theory, from which we can derive:

$$|\hat{p}_R| = \left| \frac{p_1}{\cos(\Gamma L)} \right|, \tag{20}$$

where $\hat{p}_R$ is the pressure phasor on the right side of the resonator. Figure 4 shows the result for the 1 kHz frequency. As visible on the right, the amplitude is significantly lower than for the linear

LRF model. Moreover, the wave profile is quite distorted from a pure sinusoid. Besides of a small phase shift, the 1D model matches quite closely with the 2D nonlinear simulation results.

4 CONCLUSIONS AND NEXT STEPS

We have presented a 1D numerical model to compute nonlinear viscothermal wave propagation in narrow tubes / ducts. The model is implemented in a finite element framework and has been verified using a full nonlinear compressible Navier Stokes simulation. The next steps are to compare results for axisymmetric ducts and ducts with jumps in cross sectional area jumps, to finally arrive at a model of the full BTE hearing aid system.

ACKNOWLEDGEMENTS

The authors would like to acknowledge Sonova A.G. for the financial support of this research project.

REFERENCES

[1] M. S. Alnaes, J. Blechta, J. Hake, A. Johansson, B. Kehlet, A. Logg, C. Richardson, J. Ring, M. E. Rognes, and G. N. Wells. The FEniCS Project Version 1.5. *Archive of Numerical Software*, 3(100), 2015.

[2] W. Chester. Resonant oscillations in closed tubes. *J. Fluid Mech*, 18(1):44–64, 1964.

[3] J. De Jong. *Numerical modeling of thermoacoustic systems*. PhD thesis, Universiteit Twente, Enschede, 2015.

[4] H. Haddar, J.-R. Li, and D. Matignon. Efficient solution of a wave equation with fractional-order dissipative terms. *Journal of Computational and Applied Mathematics*, 234(6):2003–2010, July 2010.

[5] H. Jasak, A. Jemcov, Z. Tukovic, and others. OpenFOAM: A C++ library for complex physics simulations. In *International workshop on coupled methods in numerical dynamics*, volume 1000, pages 1–20. IUC Dubrovnik Croatia, 2007.

[6] E. Jones, T. Oliphant, P. Peterson, and others. SciPy: Open source scientific tools for Python, 2001.

[7] L. Landau and E. Lifshitz. Fluid Mechanics, Vol. 6. *Course of Theoretical Physics*, 1987.

[8] B. Lombard and D. Matignon. Diffusive approximation of a time-fractional Burger's equation in nonlinear acoustics. *arXiv:1602.07205 [physics]*, Feb. 2016. arXiv: 1602.07205.

[9] L. Menguy and J. Gilbert. Weakly Nonlinear Gas Oscillations in Air-Filled Tubes; Solutions and Experiments. *Acta Acustica united with Acustica*, 86(5):798–810, 2000.

[10] N. Sugimoto and D. Shimizu. Boundary-layer theory for Taconis oscillations in a helium-filled tube. *Physics of Fluids (1994-present)*, 20(10), Oct. 2008.

[11] G. W. Swift. *Thermoacoustics: A unifying perspective for some engines and refrigerators*. Acoustical Society of America, Melville, NY, USA, 2003.

[12] H. Tijdeman. On the propagation of sound waves in cylindrical tubes. *Journal of Sound and Vibration*, 39(1):1–33, Mar. 1975.